International Immunology, Vol. 32, No. 1, pp. 39–48
doi:10.1093/intimm/dxz059
Advance Access publication 21 October 2019

A suppressive oligodeoxynucleotide expressing TTAGGG motifs modulates cellular energetics through the mTOR signaling pathway

Volkan Yazar[1,*], Gizem Kilic[1,*], Ozlem Bulut[1,*], Tugce Canavar Yildirim[1], Fuat C. Yagci[1], Gamze Aykut[1], Dennis M. Klinman[2], Mayda Gursel[3] and **Ihsan Gursel[1]**

[1]Thorlab-Therapeutic Oligodeoxynucleotide Research Laboratory, Department of Molecular Biology and Genetics, Faculty of Science, Ihsan Dogramaci Bilkent University, 06800 Ankara, Turkey
[2]Immune Modulation Section, Cancer and Inflammation Program, Center for Cancer Research, National Cancer Institute, Frederick, MD 21702, USA
[3]Department of Biological Sciences, Middle East Technical University, 06800 Ankara, Turkey

Correspondence to: I. Gursel, Thorlab-Therapeutic Oligodeoxynucleotide Research Laboratory, Department of Molecular Biology and Genetics, Faculty of Science, Ihsan Dogramaci Bilkent University, Building B, Room 244, 06800 Ankara, Turkey; E-mail: ihsangursel@bilkent.edu.tr

*These authors contributed equally.

Received 11 February 2019, editorial decision 21 August 2019; accepted 20 September 2019

Abstract

Immune-mediated inflammation must be down-regulated to facilitate tissue remodeling during homeostatic restoration of an inflammatory response. Uncontrolled or over-exuberant immune activation can cause autoimmune diseases, as well as tissue destruction. A151, the archetypal example of a chemically synthesized suppressive oligodeoxynucleotide (ODN) based on repetitive telomere-derived TTAGGG sequences, was shown to successfully down-regulate a variety of immune responses. However, the degree, duration and breadth of A151-induced transcriptome alterations remain elusive. Here, we performed a comprehensive microarray analysis in combination with Ingenuity Pathway Analysis (IPA) using murine splenocytes to investigate the underlying mechanism of A151-dependent immune suppression. Our results revealed that A151 significantly down-regulates critical mammalian target of rapamycin (mTOR) activators (*Pi3kcd*, *Pdpk1* and *Rheb*), elements downstream of mTOR signaling (*Rps6ka1*, *Myc*, *Stat3* and *Slc2a1*), an important component of the mTORC2 protein complex (*Rictor*) and *Mtor* itself. The effects of A151 on mTOR signaling were dose- and time-dependent. Moreover, flow cytometry and immunoblotting analyses demonstrated that A151 is able to reverse mTOR phosphorylation comparably to the well-known mTOR inhibitor rapamycin. Furthermore, Seahorse metabolic assays showed an A151 ODN-induced decrease in both oxygen consumption and glycolysis implying that a metabolically inert state in macrophages could be triggered by A151 treatment. Overall, our findings suggested novel insights into the mechanism by which the immune system is metabolically modulated by A151 ODN.

Keywords: A151 ODN, immunometabolism, immunosuppression, microarray

Introduction

The immune system evolved to protect the host from pathogenic insult, but uncontrolled inflammation can be harmful, as in the case of autoimmunity (1). Indeed, immune responses are typically down-regulated as part of the physiologic processes associated with tissue remodeling during the resolution phase of inflammation. It was recently shown that DNA released by dying host cells contains immunosuppressive elements capable of down-regulating over-active immune responses (2, 3). The repetitive TTAGGG motifs present in mammalian telomeres dominate this immunosuppression, an effect that can be mimicked using synthetic $TTAGGG_4$ oligodeoxynucleotides (ODNs) (4, 5). $TTAGGG_4$ (referred to as A151) was shown to inhibit the production of numerous chemokines and cytokines triggered by bacteria including but not limited to IL-6, IL-12, IFNγ, TNFα and MIP2α (5, 6). A151 is thus the archetypal immunosuppressive ODN and a promising therapeutic candidate (2), yet its effect on the transcriptome of immune cells remains a mystery.

Mammalian target of rapamycin (mTOR) is the key element that integrates a variety of signaling pathways sensing cellular

stress, nutrient levels and energy status (7). It mainly acts by forming two complexes: mTORC1 and mTORC2 that have different roles in health and disease. mTOR activation regulates many cellular processes including autophagy, survival, cell growth and proliferation (8). Accumulating data in recent years revealed that metabolic reprogramming involving the mTOR pathway is critical for immune cells to adapt to rapidly changing environmental conditions and optimize their effector responses. Activated immune cells mainly increase glycolysis and anabolic metabolism through mTOR activity to meet the high energy needs required for effector function (9). For instance, mTOR deficiency led impaired differentiation of naive T cells to T_h1, T_h2 and T_h17 cells even in the presence of polarizing factors while promoting $Foxp3^+$ regulatory T-cell (Treg) generation. Defective effector cell differentiation was associated with decreased STAT4, STAT6 and STAT3 activities (10). Although downstream effects of mTOR activation or inhibition on T cells is more clearly defined, studies investigating the role of mTOR signaling in macrophage activity and metabolism reveal a more complex regulatory network involving both mTORC1 and mTORC2. As an example, deletion of TSC1, a negative regulator of mTORC1 and mTORC2, enhanced M1 polarization with increased pro-inflammatory cytokine production while reducing IL-4 induced anti-inflammatory M2 polarization (11).

This work was undertaken to generate a complete and reliable list of genes whose expression levels are significantly altered by immunosuppressive ODN treatment. Towards that end, a comprehensive microarray analysis in combination with Ingenuity Pathway Analysis (IPA) was performed to investigate the effect of A151 on the immune cell transcriptome in mice. These results indicated that A151 might have a profound impact on mTOR-dependent metabolic activities, a finding which might explain the mechanism by which A151 ODN functions. We validated this hypothesis by investigating A151's effect on mTOR phosphorylation levels, oxygen consumption and glycolytic capacity in macrophages. Outcomes of this study provide new insights on the mechanisms of clinically useful DNA-based immunosuppressive agents and open up a novel therapeutic potential for their use as metabolic regulators.

Methods

Microarrays

Seventy-six microarrays were kept in the mAdb database (Microarray Database, a collaboration of CIT/BIMAS and NCI/CCR at the NIH) and formatted via the export function for use with BRB ArrayTools. In our experimental setting, each data set represents a different time point in a time-course experiment at 1, 2, 4 and 8 h post-exposure (at each time point with minimum 3 up to 11 biological replicate arrays per treatment group): (i) control ODN, (ii) CpG alone as an immunostimulatory ODN and (iii) A151 alone as an immunosuppressive ODN. Of 76 microarray platforms, a total of 44 chips [of experiments at 2 and 8 h post-exposure for all groups included, as suggested in literature (3, 15, 16)] were prioritized to investigate further after differential expression analyses within the scope of this study.

Differential expression analysis

The signal-to-noise ratio of data sets was calculated with mAdb. Reproducibility was established after gene expression profiles of similarly treated cultures from independent experiments were benchmarked against each other. Differential expression analyses of multiple microarray data were performed using BRB-ArrayTools (https://brb.nci.nih.gov/BRB-ArrayTools/). Data were background corrected, flagged values were excluded, spots with both signals below 100 were removed, ratios were log base 2 transformed, and Lowess-intensity dependent normalization was leveraged to adjust for differences in labeling intensities of the Cy3- and Cy5-dyes (12). Only genes present on >50% of the arrays after filtering were included in the subsequent analyses. Genes were filtered out if <20% of their expression data values have at least a 1.5-fold change in either direction from the gene's median value, which in turn resulted in removal from downstream analysis of up to 85% of all genes represented on an array.

Genes that show patterns of differential expression in treatment groups were identified using a random-variance *t*-test within the frame of Class Comparison analysis by BRB-ArrayTools. The random-variance *t*-test is an improvement over the standard separate *t*-test as it permits sharing information among genes about within class variation without assuming that all genes have the same variance (13). Genes were considered statistically significant if their *P* value was <0.0001 (BRB Manual, Sample Statistical Methods Descriptions). Differences between groups in terms of number of genes regulated were established by chi-squared analysis and Fisher's exact test (14).

Pathway analysis

IPA software (QIAGEN®, https://www.qiagenbioinformatics.com/products/ingenuity-pathway-analysis) was used for the functional interpretation of differential expression results obtained from the aforementioned microarray analyses. The network explorer of IPA was used to identify interactions among the genes supplied and using these to generate gene–gene interaction networks (GGINs) with shortest literature-supported paths (edges) between genes (nodes). The statistical significance for each assignment was expressed by a corresponding *P* value calculated using Fisher's exact test.

Reagents

CpG ODN, 1555: 5′-GCTAGACGTTAGCGT-3′, Control ODN, 1612: 5′-GCTAGAGCTTAGCGT-3′ and Suppressive ODN, A151: 5′-TTAGGGTTAGGGTTAGGGTTAGGG-3′, Control Suppressive ODN: 5′-TTACCC-TTACCCTTACCCTTACCC-3′ sequences were all modified with a phosphorothioate backbone and obtained either from Alpha DNA (Montreal, Quebec, Canada) or from CBER/FDA, ODN Core Facility (Bethesda, MD, USA). All cell culture media components were from Thermo Fisher (Waltham, MA, USA) and Biological Industries (Cromwell, CT, USA). qRT-PCR primers and flow cytometry antibodies are given in Supplementary Tables 1 and 2, respectively.

Bone marrow-derived macrophage generation

Femur and tibia bones of 6–8 weeks old C57BL/6 mice were removed, two ends of the bones were cut, and bone marrow was obtained by flushing out cell culture media through the bone with a syringe. Cells were washed with cell culture media, centrifuged at 300 RCF for 5 min, re-suspended with ACK Lysis Buffer (Lonza, Basel, Switzerland) and washed again after 30 s. Cells were seeded on low-attachment 24-well plates as 5×10^5 cells per well in 30% L929 conditioned medium containing macrophage colony-stimulating factor (M-CSF). Seven days later, cells were collected, and macrophage marker expressions were analyzed with a NovoCyte 3000 flow cytometer (ACEA Biosciences, San Diego, CA, USA).

Cell culture and stimulations

For qRT-PCR analyses, splenocytes isolated from 10- to 12-week-old male BALB/c mice were seeded at 6×10^6 cells ml^{-1} density and stimulated with 1 μM 1555, 1612 and 1 μM or 3 μM A151 for 8 h. For flow cytometry studies, mouse peritoneal exudate cells (PECs) were collected from male 8- to 10-week-old C57BL/6 mice by injecting 10 ml phosphate-buffered saline (PBS) into the peritoneal cavity and collecting the fluid. Bone marrow-derived macrophages (BMDMs) and PECs were seeded at 4×10^5 cells per well density in 96-well plates and stimulated with 100 ng ml^{-1} lipopolysaccharide (LPS) from *Escherichia coli* O55:B5 (Sigma-Aldrich, St. Louis, MO, USA) and/or 100 nM rapamycin (Invivogen, San Diego, CA, USA) in the presence or absence of 3 μM A151 for 1 h. A151 was either given 4 h before LPS and rapamycin administration or simultaneously. After 1 h of LPS/rapamycin incubation, cells were collected and stained for phosphorylated mTOR. For immunoblotting experiments, BMDMs were seeded at 2×10^6 cells ml^{-1} in 60 mm × 15 mm petri dishes and stimulated with 100 ng ml^{-1} LPS and/or 100 nM rapamycin in the presence or absence of 3 μM A151 for 1 h. A151 was given 4 h before LPS and rapamycin. After 1 h of LPS/rapamycin incubation, cells lysates were collected.

All cells were cultured in RPMI 1640 supplemented with 5% fetal bovine serum (FBS), 2 mM L-glutamine, 10 mM HEPES, 1 mM Na-Pyruvate, 50 μg ml^{-1} penicillin/streptomycin and incubated at 37°C in a 5% CO_2 incubator.

Total RNA extraction and quantitative real-time polymerase chain reaction

Total RNA from splenocytes was extracted using TRIzol reagent (Invitrogen, Carlsbad, CA, USA) according to the manufacturer's protocol. Reverse transcription was done with the RevertAid RT Reverse Transcription Kit (Thermo Fisher, Waltham, MA, USA). Quantitative real-time polymerase chain reaction (qRT–PCR) reactions were performed with a Light Cycler 480 SYBR Green I Master (Roche, Basel, Switzerland) as per the manufacturer's instructions. PCR primers are provided in Supplementary Table 1.

Intracellular staining for mTOR phosphorylation

Cells were precipitated and re-suspended with BD Biosciences Phosflow Lyse/Fix Buffer (San Jose, CA, USA) and incubated for 10 min at 37°C. After 10-min centrifugation at 600 RCF, the pellet was washed with PBS and centrifuged again. Cells were re-suspended in cold 90% methanol and incubated for 30 min on ice. After washing twice and centrifugation at 600 RCF for 10 min, cells were incubated with fluorochrome anti-F4/80, anti-CD11b, anti-B220 and anti-TCRb and anti-p-mTOR antibodies for 1 h at room temperature. After incubation, cells were washed again with PBS once and analyzed with flow cytometry. Details about the antibodies are provided in Supplementary Table 2.

Immunoblotting analysis

Cell lysates were incubated with RIPA buffer containing 2 M NaCl, 1 M Tris (pH = 8), NP-40, 10% SDS, protease inhibitor cocktail (Thermo Fisher) and phosphatase inhibitors (Thermo Fisher). After 30 min of incubation with intermittent vortexing every 5 min, lysates were centrifuged at 10 000 RCF for 20 min, and supernatants were collected. Twenty-five micrograms of protein were loaded per well and separated by 7% sodium dodecyl sulfate–polyacrylamide gel electrophoresis (SDS–PAGE), transferred to a PVDF membrane and probed with 1:1000 diluted primary antibodies against β-actin, mTOR, STAT3, p-mTOR and p-STAT3. Blots were visualized by an Amersham Imager 600 (Little Chalfont, UK) after incubating the membranes with 1:5000 diluted HRP-linked secondary antibodies. Details on all antibodies are given in Supplementary Table 3.

Metabolic assays

BMDMs were seeded at 3×10^4 cells per well in Seahorse XFp Cell Culture Miniplates and incubated overnight at 37°C in a 5% CO_2 incubator. The next day, cells were stimulated with 3 μM A151 ODN for 4 h, then the medium was replaced by Seahorse XF Assay Medium, and cells were incubated for 1 h at in 37°C in a non-CO_2 incubator. The oxygen consumption rate (OCR) and extracellular acidification rate (ECAR) were measured using a Seahorse Bioscience XFp Extracellular Flux Analyzer and Glycolytic Rate Assay Kit (Billerica, MA, USA).

Statistical analysis

Statistical significances were analyzed with GraphPad Prism V7 software (San Diego, CA, USA) using Student's *t*-test, one-way analysis of variance (ANOVA) followed by Dunnett's multiple comparison test or two-way ANOVA followed by Sidak's multiple comparison test. *P* values <0.05 were considered significant.

Results

A151 has a global effect on gene expression in mouse splenocytes

Transcriptome profiling of mouse splenocytes treated with immunosuppressive A151 ODN or immunostimulatory CpG ODN was performed using microarray technology as described above, which enabled us to gain insight into the changes in expression patterns of mouse genes in response to varying immunomodulatory ODN treatments. In comparison of the A151 treatment group with the control ODN treatment group, we produced a list of 1276 differentially expressed genes (DEG-1; Supplementary File 3), of which 814 genes were found down-regulated. Another list of DEGs was

obtained when the A151 treatment group was compared with the CpG ODN treatment group; of 1541 DEGs identified, 1063 genes were found down-regulated (DEG-2; Supplementary File 4). As a proof-of-concept experiment of the feasibility of our methodology, we then compared the CpG treatment group with the control group to check to see if the marker genes of this well-established immunostimulatory ODN would be up-regulated or not; in a list of 459 DEGs, 261 genes, including CpG marker genes, were identified up-regulated (DEG-3; Supplementary File 5). Subsequently, a Venn diagram to identify both common and unique genes across each of these three gene lists was plotted (Fig. 1A); a vast number of genes (492) exclusive to A151 treatment (Control_vs_A151) were found differentially expressed. A total of 117 genes (66 + 51) were identified differentially expressed after CpG ODN treatment and A151 treatment separately (i.e. Control vs CpG and Control vs A151), 66 of which were found down-regulated in all pairwise comparisons. We further scrutinized the region (667 DEGs) that is displayed in the diagram as the intersection between CpG versus A151 and Control versus A151 and that is excluded by common genes across all pairwise comparisons. Normalized intensity of expression of the genes that yielded the aforementioned Venn diagram is illustrated in a heat map (Fig. 1B). Taken together, it was observed that A151 has a profound down-modulatory impact on the transcriptome of mouse splenocytes globally.

GO analysis and IPA correlates with metabolic processes

A subsequent GO term analysis (http://geneontology.org/page/go-enrichment-analysis) helped us in sorting these 667 genes with respect to the biological processes they involve; in addition to the already known impact of A151 on the immune system (2), we defined main categories as 'Metabolic Processes', 'Mitochondrion Organization', 'MAP Kinase Activity', 'Apoptosis and Cell Cycle Control' or, 'Transcription by RNAPII'. As most of these categories either directly or indirectly relate to cellular energetics, we moved along that axis and decided to analyze in our final gene list the expression status of the genes that involve the mTOR signaling pathway, the master regulator of cell metabolism, growth, proliferation and survival. For the sake of reproducibility, the actual intensities of 23 mTOR-related genes are represented in a heat map using time-course expression data (Fig. 1C). A151 treatment appeared to severely down-regulate 22/23 genes. The genes within the categories relevant to metabolic processes were used to produce individual GGINs through IPA (Supplementary Figure 1), which allows for identification of network/pathway interactions among genes with each gene's change in direction of expression all accounted for. The GGIN of mTOR-related genes obtained within our final list yielded a true reflection of the original pathway itself (Fig. 2 and Supplementary Figure 1A). Overall, A151 ODN appeared to involve mTOR-dependent metabolic regulation.

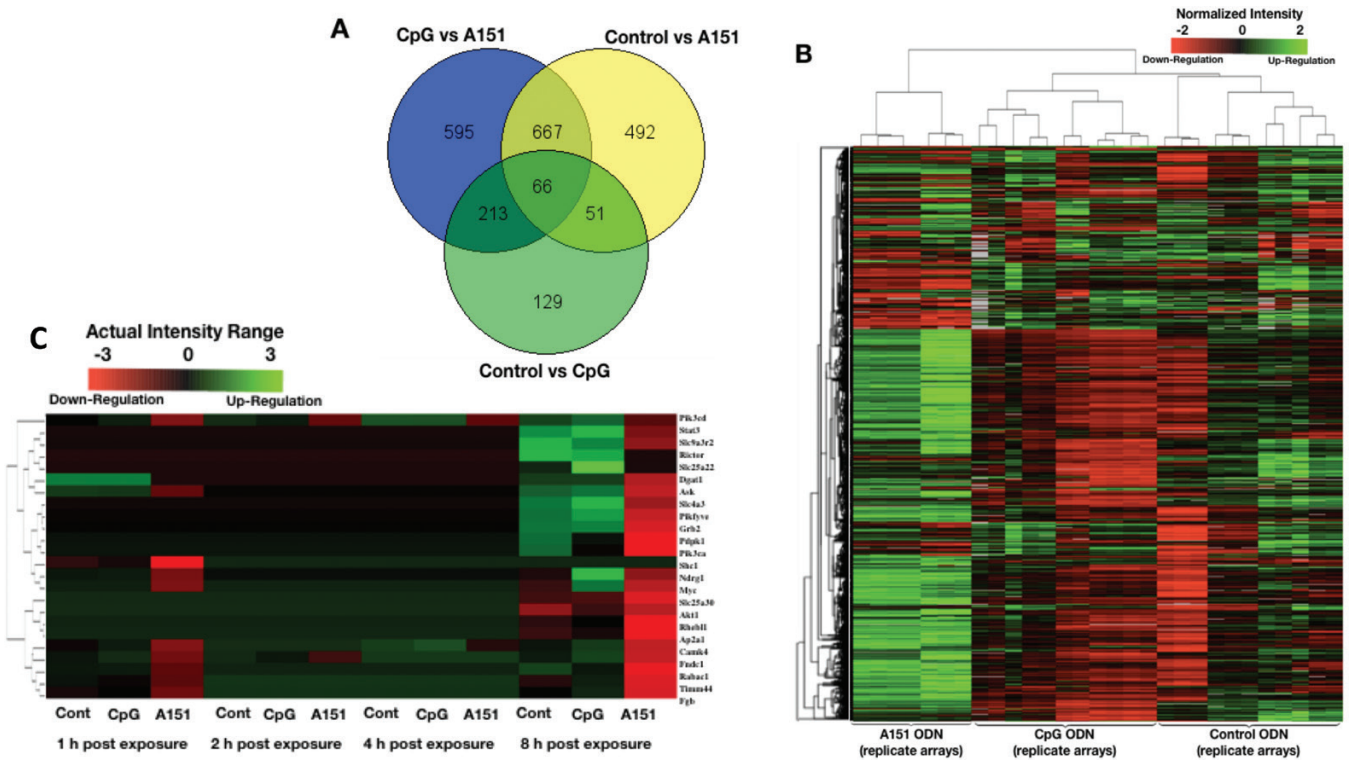

Fig. 1. Comprehensive microarray analysis of murine splenocytes for A151, CpG and control ODN treatment groups at 8 h post-exposure. (A) Venn diagram showing both common and unique genes across each of the gene lists obtained from different pairwise group comparisons. (B) The heat map that illustrates normalized intensity of expression of the genes that yielded the Venn diagram in panel (A). Time- and treatment-dependent hierarchical analysis of expression levels of mTOR-related genes. (C) The heat map that illustrates for the purpose of reproducibility the 'actual' mean intensities of 23 mTOR-related DEGs across all time points tested.

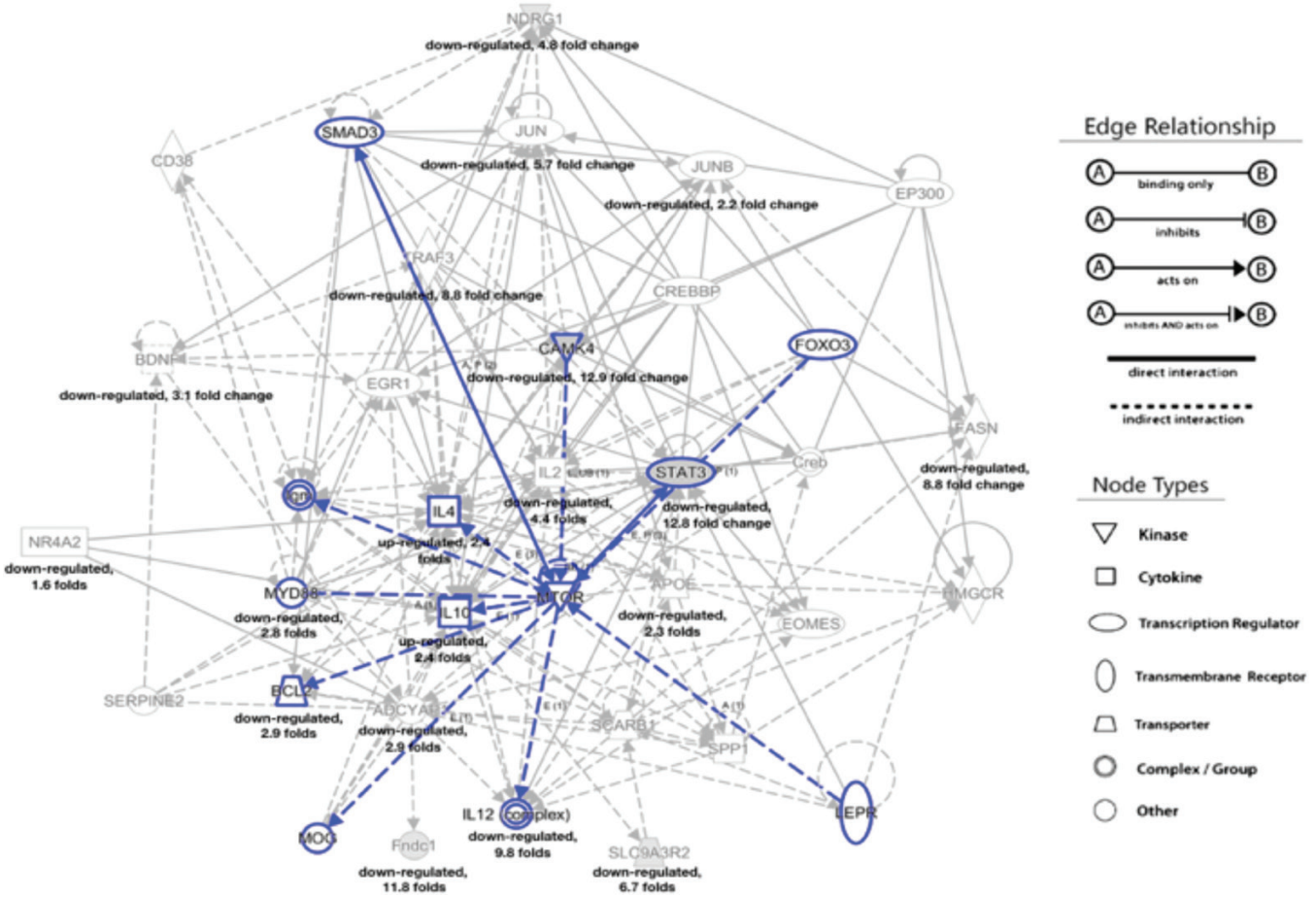

Fig. 2. The GGIN identified by IPA software. The input was the list of 23 mTOR-related genes described in Fig. 1(C). Imported gene identifiers were mapped to corresponding gene objects and overlaid onto the global molecular network identified by the IPA algorithm. Edge relationship and node type symbols illustrate the nature of the relationship among genes, considering the functionality of each gene supplied. Solid lines: direct interaction. Dashed lines: indirect interaction. Shaded nodes: the genes present in the input list. Empty nodes: the genes inserted after high confident prediction by the IPA algorithm. Fold changes and changes in expression pattern were calculated based on A151 treatment.

RT–qPCR validates the microarray results revealing down-regulation in mTOR-related genes

Within these 23 genes belonging to the mTOR signaling pathway in our final list, we selected for validation 6 genes yielding, after treatment, distinct expression patterns in microarray data. We also decided to investigate the expression profile of other chief mTOR markers that did not show up in our data sets, including *Rpska1*, *Slc2a1* and *Mtor*. Validation of microarray results was done using qRT-PCR for the selected group of genes. Similar to the microarray data sets which consist of mouse splenocyte samples, we stimulated BALB/c splenocytes with CpG ODN 1555 and A151 ODN either alone or in combination for 2 and 8 h, as suggested in literature (3, 16). Neither CpG nor A151 resulted in significant changes in gene expression after 2 h of incubation (Supplementary Figure 2). In contrast, after 8 h post-exposure, A151 both in the absence and in the presence of CpG ODN decreased the expression of *Pi3kcd*, *Pdpk1* and *Rheb*, all of which are well-known upstream regulators of mTOR (Fig. 3A–C). Furthermore, A151 down-regulated mTOR itself although less significantly (Fig. 3D). The expression of *Rps6ka1*, *Myc*, *Stat3* and *Slc2a1* was significantly reduced after A151 treatment regardless of CpG treatment (Fig. 3E–H). S6 kinase alpha-1 coded by *Rps6ka1*, GLUT1 coded by *Slc2a1*, Stat3 and Myc are all downstream targets of mTOR (18, 20, 24). Of note, CpG ODN alone highly up-regulated *Stat3* expression, and A151 treatment was sufficient to inhibit its expression back to even less than the basal level (Fig. 3G). Moreover, *Rictor*, an essential component of the mTORC2 complex, was also found to be down-regulated after 8 h of 3 μM A151 exposure (Fig. 3I). The A151 effect appeared to be dose-dependent for all the genes involved. While 1 μM A151 had no effect or a moderate effect, 3 μM A151 was able to down-regulate expression of these mTOR-related genes consistently. Taken together, qRT-PCR results are in accord with the outcome of the microarray analyses (Figs 1C versus 2).

A151 ODN inhibits mTOR phosphorylation in macrophages and B cells

To confirm as to whether A151 modulates the activity of mTOR at the protein level as well, we next analyzed mTOR phosphorylation via flow cytometry and immunoblotting. For flow cytometry analysis, A151 ODN stimulation was done either 4 h before LPS treatment or together with LPS treatment because A151 exerts its immunomodulatory effect

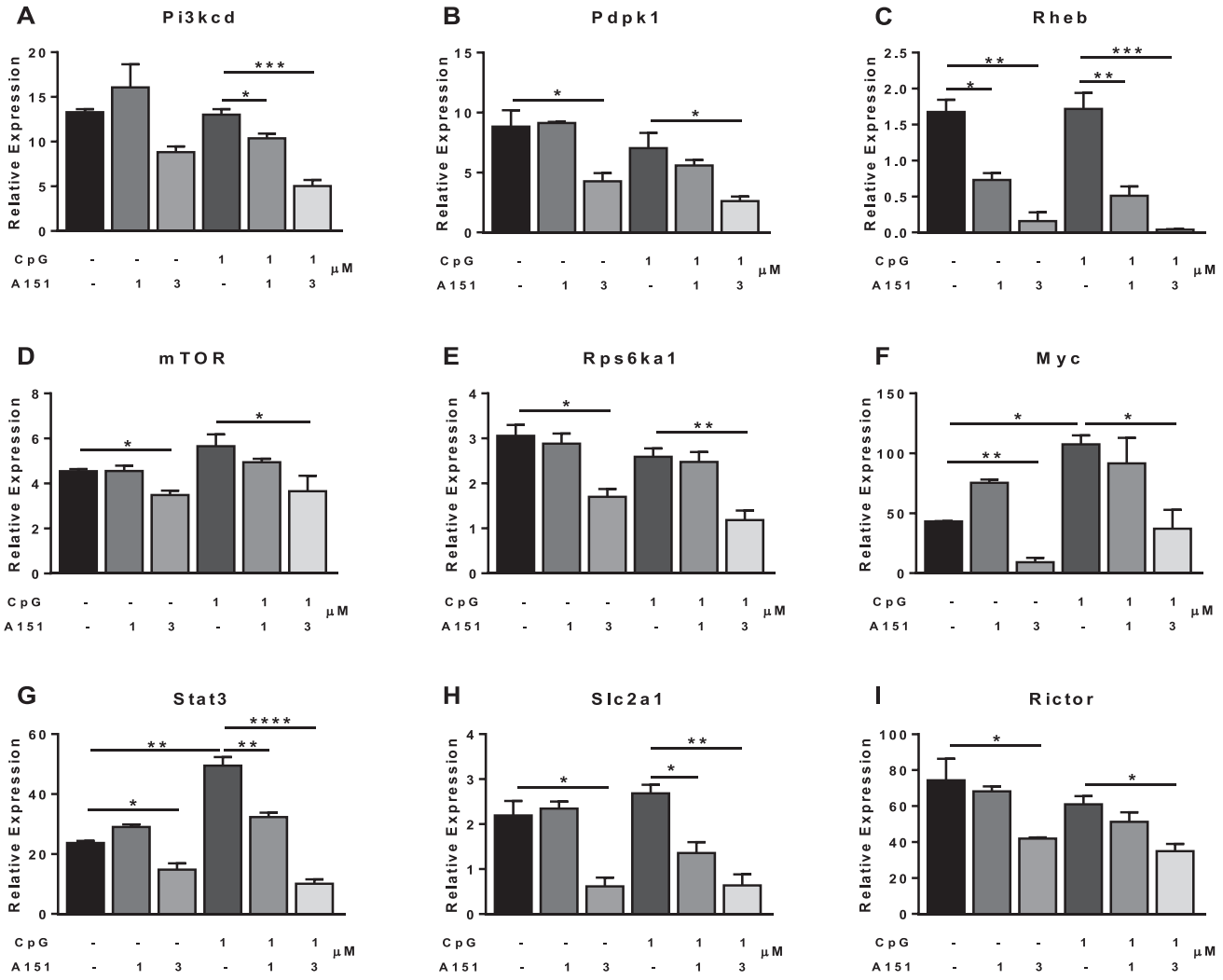

Fig. 3. Effect of A151 treatment on components of the mTOR signaling pathway in mouse splenocytes. Effects of 1555 CpG ODN and A151 on the mRNA levels of (A) *Pi3kcd*, (B) *Pdpk1*, (C) *Rheb*, (D) *mTOR*, (E) *Rps6ka1*, (F) *Myc*, (G) *Stat3*, (H) *Slc2a1* and (I) *Rictor* relative to β-actin were determined with qRT–PCR using an efficiency corrected comparative *CT* method after cells were stimulated for 8 h in culture. Data are the average of three independent experiments run in triplicates and are represented as mean ± SEM. *$P \leq 0.05$, **$P \leq 0.01$, ***$P \leq 0.001$, ****$P \leq 0.0001$.

after the cellular uptake, which takes about 2–4 h (5). The phosphorylation level was assessed after 1 h of LPS stimulation. We found that A151 mildly decreased mTOR phosphorylation in BMDMs when administered simultaneously with LPS, whereas A151 addition to culture media 4 h earlier led to a striking decrease ($P < 0.01$) in mTOR phosphorylation (Fig. 4A). A151 ODN treatment also reduced mTOR phosphorylation in the absence of LPS, although not significantly. Similarly, A151 prevented mTOR phosphorylation in LPS-stimulated macrophage and B-cell populations in PECs (Fig. 4B). Furthermore, we revealed that A151 is as effective as the widely used mTOR inhibitor rapamycin (Fig. 4A–C).

We further confirmed inhibition of mTOR phosphorylation by A151 performing immunoblotting with BMDMs. Since A151 had proved to be more effective when it was administered 4 h before mTOR activation with LPS, we did not include simultaneous A151 addition for this experiment. Although A151 ODN did not cause any alterations in total mTOR and STAT3 protein levels, it decreased their phosphorylation induced by LPS (Fig. 4C). Collectively, our data demonstrated that A151 plays an inhibitory role in post-transcriptional regulation of mTOR, as well as its down-regulatory effect on mTOR at the transcriptional level.

A151 shifts macrophages to a metabolically quiescent state reducing glycolysis and oxygen consumption

We investigated the metabolic profiles of cells treated with A151 using a Seahorse Analyzer (Fig. 5). Upon A151 but not Control A151 ODN treatment for 4 h, basal ECARs and OCRs were followed for 90 min. A151 treatment resulted in lower ECAR (Fig. 5A) and OCR (Fig. 5B) compared to the untreated or Control ODN. The results imply that A151 shifts these BMDMs to a more metabolically quiescent state by reducing the major routes of energy production namely glycolysis and oxidative phosphorylation.

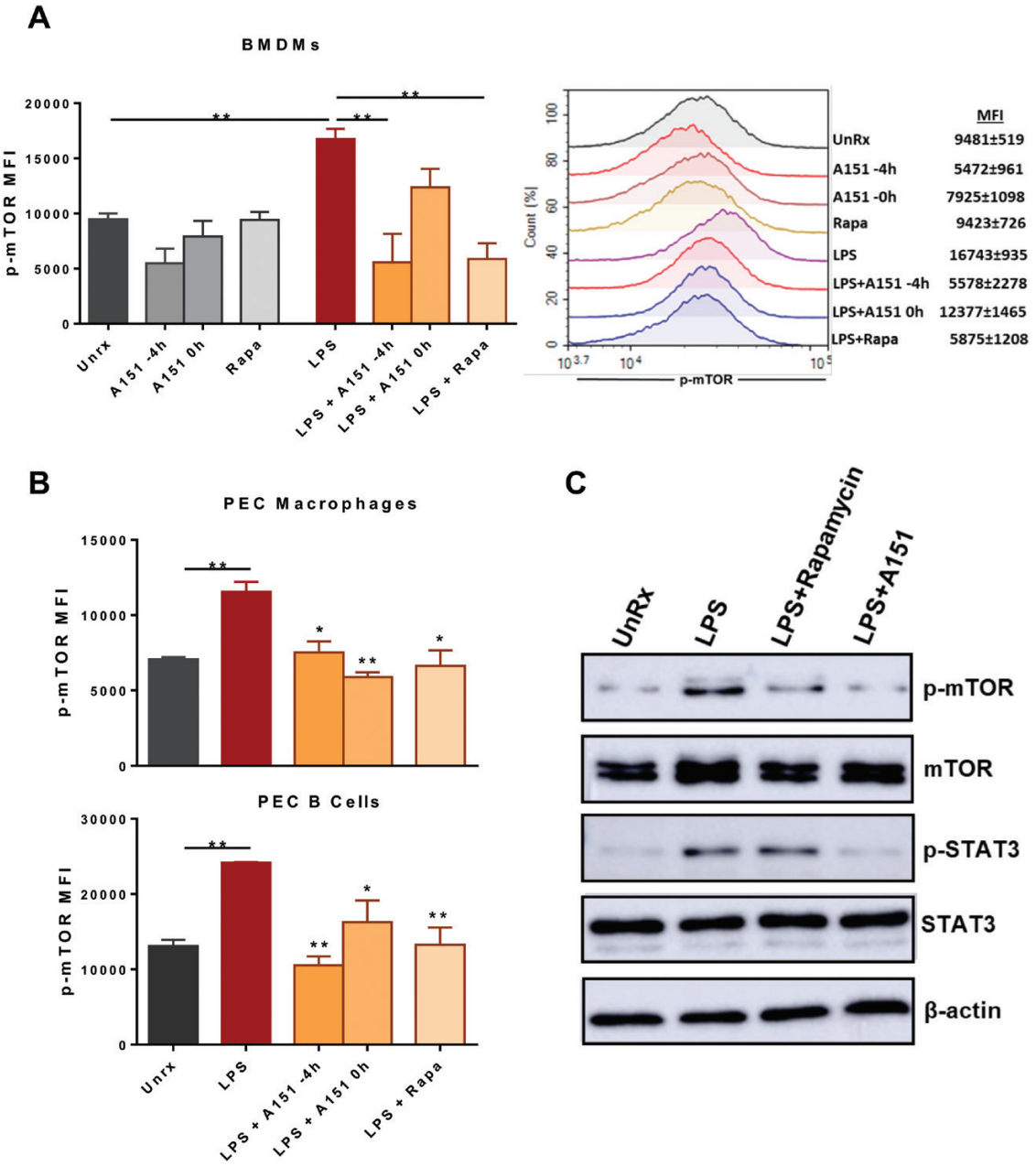

Fig. 4. Effect of A151 treatment on mTOR phosphorylation in mouse macrophages and B cells. (A) Quantification of p-mTOR fluorescence intensities (left) and a representative histogram plot (right) in mouse BMDMs. (B) p-mTOR fluorescence intensities in macrophages (top) and B lymphocytes (bottom) in PECs. Cells were incubated with LPS (100 ng ml^{-1}) or rapamycin (100 nM) in the presence or absence of A151 (3 μM) for 1 h. A151 was either given 4 h before (−4 h) LPS and rapamycin administration or simultaneously (0 h). CD11b^{+}, F4/80^{+} macrophages and TCRβ-B220^{+} B-cell populations in PECs were analyzed separately. (C) Protein levels of total and phosphorylated mTOR and STAT3 were determined by immunoblotting. A151 was given 4 h before 1-h incubation with LPS or rapamycin. Data are average of three independent experiments run in triplicates and are represented as mean ± SEM. Unrx: untreated control, Rapa: rapamycin, MFI: mean fluorescence intensity. *$P \leq 0.05$, **$P \leq 0.01$.

Discussion

Mammalian telomeric ends expressing TTAGGG repeats (mimicked using a synthetic ODN named as A151) suppress immune responses and contribute to the fine-tuning of immune homeostasis (17). Yet, the down-modulatory mechanism of A151 action is very limited and its modus operandi at the gene level remains unresolved. Additionally, the degree, duration and breadth of A151-induced alterations in the immune transcriptome appear partially understood (2). Given the medical potential A151 holds for immunosuppressive therapy in humans as a 'self-biomolecule' (2, 5, 17), understanding the underlying molecular mechanisms via which A151 operates is invaluable. Towards that end, we attempted to uncover the mystery lying behind A151's effects on the

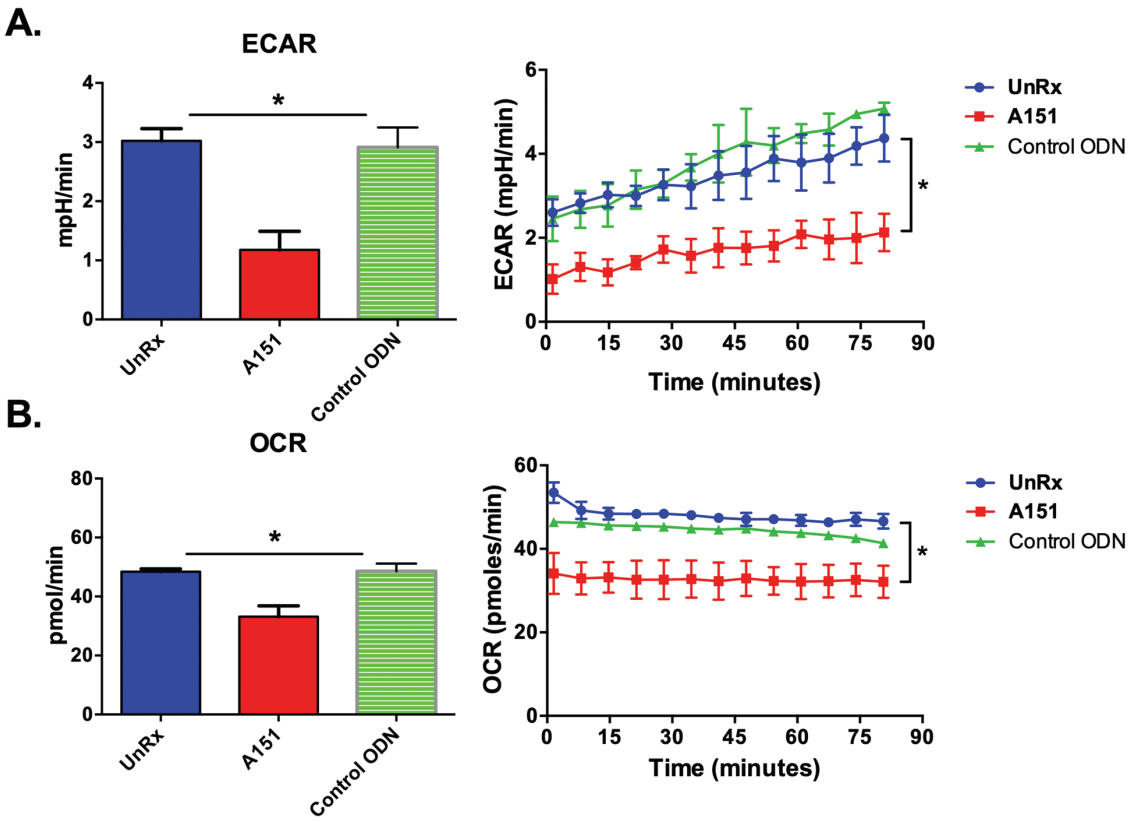

Fig. 5. Changes in metabolic activity caused by A151 ODN in mouse macrophages. BMDMs were either left unstimulated or incubated either with Control A151 or A151 ODN for 4 h, then re-plated in Seahorse assay medium. (A) ECAR and (B) OCR were measured by a Seahorse Analyzer for 90 min following 4 h of incubation. Data are the average of two independent experiments run in triplicates and are represented as mean ± SEM. Unrx: untreated control. *$P \leq 0.05$.

immune cell transcriptome using a comprehensive analysis approach for our in-house microarray data sets within the scope of this study.

A widely observed yet perplexing phenomenon in A151 studies, once immune cells are treated with A151, is a state of reluctance in the cultured cells, implying the onset of cellular anergy. Considering the notion that cellular energetics play a pivotal role in immune cell function and that the mTOR signaling pathway serves as the master regulator of cell metabolism, growth, proliferation and survival, we decided to scrutinize the expression status of mTOR mediators within our data sets (Fig. 1C). We discovered at the transcriptome level that many well-known mTOR-related proteins, including Stat3 (18), Pi3kcd (19), Myc (20), Rictor (21), Pdpk1 (22), Akt1 (23) and Rhebl1 (24), were found consistently down-regulated (fold changes 11.8, 5.9, 2.2, 2.1, 2, 2, 2.9, respectively) in A151 treatment groups (particularly at >4 h post-exposure). This observation was then physically validated, along with other chief mTOR markers that 'did not' show up in our data sets (Fig. 3). Interestingly, no such effect of A151 on the mTOR pathway was noted at an earlier time point (Fig. 1C and Supplementary Figure 2). An interesting point of discussion is that, since we are experiencing a down-modulatory A151 effect on the mTOR pathway mostly at 8 h post-exposure but not at 2 h after incubation, could this impact on mTOR be an epiphenomenon rather than primary? In other words, if A151 is shutting down metabolically active immune cells via some other mechanism initially, a natural consequence would be a reduction in the expression of the genes that mediate cellular metabolism afterwards. We are currently investigating this possibility with various functional assays.

The IPA-identified GGINs of mTOR-related genes yielded a true reflection of the original pathway itself, placing mTOR to the center as the chief regulator of the interaction network (Fig. 2). Ultimately, we managed to obtain a group of GGINs that yield a whole list of direct and indirect interactions of all 23 mTOR-related genes (Fig. 1C) in our data sets. Some of the most informative networks are given in Supplementary Figure 1. That a good deal of these interactions are indirect means there is more to uncover regarding the involvement of A151 in cellular energetics, yet this still is a good point to begin with. Of note, the transcriptome data revealed that the CpG ODN exerted an opposite effect on expressions of some mTOR-related genes, such as *Stat3* and *Myc* (Fig. 3), just as expected given the CpG-led massive cytokine storm immune cells need to fuel; however, our data implicated that mTOR activation is not involved in BMDMs (data not shown). Although we observed that *Rictor* is down-regulated both in transcriptome analysis and qRT–PCR, how A151 ODN alters mTORC1/2 function deserves further investigation.

The knowledge that mTOR needs phosphorylation to become functionally active was leveraged to further validate the A151 effect on mTOR activity. Phosphorylation of mTOR was abrogated after A151 treatment, as visible in flow cytometry

and immunoblotting experiments (Fig. 4), particularly when cells were pre-treated with A151 before induction of mTOR phosphorylation with LPS. This suggests that the inhibitory effect of A151 on mTOR is observed not only at the transcriptional level but also at the post-transcriptional level. In fact, A151 was observed to be as potent as rapamycin, which is the gold-standard mTOR inhibitor (Fig. 4A–C).

Upon the observation of down-regulation in *Slc2a1* coding for glucose transporter GLUT1 by A151, we hypothesized that A151 ODN might decrease glucose intake and hence the hence glycolytic capacity of macrophages. Of note, GLUT1-dependent glucose uptake is crucial for macrophage activation and pro-inflammatory phenotype (25). Surprisingly, besides a decrease in glycolytic capacity, we observed a significant reduction in oxygen consumption revealed by metabolic assays (Fig. 5). The hypo-responsive anergic state of T cells is characterized by low mTOR activity and metabolic deficiency (26). Consistent with the literature findings on T cells, our data suggest a similar metabolically inert state in macrophages triggered by A151 ODN. It might be of great interest to investigate whether A151 through similar pathways drives T-cell anergy.

Figure 4B reveals that A151 can inhibit mTOR phosphorylation not only in macrophages but also in B cells. mTOR signaling is critical for B-cell function. The mTOR inhibitor rapamycin was found to inhibit proliferation of B cells and their differentiation to antibody-producing cells while arresting the cell cycle progression at the G1 phase (27). Moreover, mice with reduced mTOR production due to a hypomorphic allele have reduced B-cell numbers, decreased antibody production, reduced migration in response to chemokines and impaired development at the pre-B-cell stage (28). Also, aberrant mTOR activation is observed in many B-cell malignancies such as B-cell acute lymphoblastic leukemia and mantle cell lymphoma (29). These observations resulted in numerous clinical trials utilizing mTOR inhibitors alone or in combination with other therapeutic approaches for the treatment of these malignancies. A151 ODN's potential as an mTOR inhibitor might be relevant in such clinical settings. Since A151 has been shown to inhibit B-cell proliferation, activation and IgE, IgA, IgG1 and IgG4 production in humans (30), it now seems plausible that this modulation of B-cell functions might be mTOR-dependent.

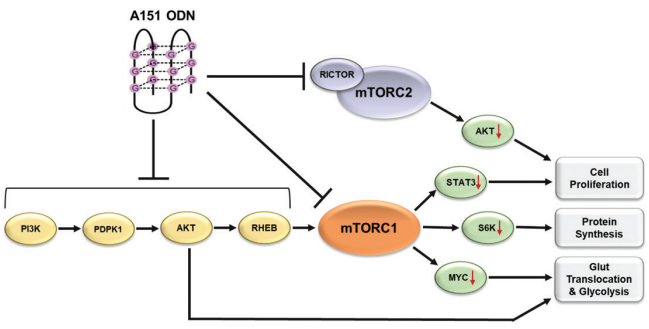

Fig. 6. A novel universal mechanism of immunosuppressive A151 ODN. Microarray transcriptome analyses, flow cytometric investigations, immunoblotting and qPCR experiments collectively revealed that immunosuppressive A151 ODN down-regulates PI3K/AKT pathway elements, mTOR complexes and their downstream targets.

Consequently, microarray transcriptome analyses, flow cytometric investigations, immunoblotting and qRT–PCR experiments consistently revealed that immunosuppressive A151 ODN down-regulates PI3K/AKT pathway elements, mTORC1/2 and their downstream targets (Fig. 6). This could be a unifying mechanism of action of A151 ODN through regulating the cellular energetics of the immune cells. The extent of the distinct response(s) of naive or activated cells to this stimulus is currently under investigation.

Funding

This work was partially supported by the Scientific and Technological Research Council of Turkey (TUBITAK) (grant number: 115S492 to I.G.), (grant number: 115S837 to I.G.) and the Ministry of Development (grant name: UMRAM-ASI, project #: 2015BSV302 to I.G.).

Acknowledgements

The authors appreciate Mr Ulas Sacinti for the help in care and handling of experimental animals used throughout this study.

Conflicts of interest statement: The funders had no role in study design, data collection, decision to publish or preparation of the manuscript. The authors (I.G., M.G., D.M.K.) declare that they have inventor rights on A151-related patents.

References

1 Klinman, D. M., Gursel, I., Klaschik, S., Dong, L., Currie, D. and Shirota, H. 2005. Therapeutic potential of oligonucleotides expressing immunosuppressive TTAGGG motifs. *Ann. N. Y. Acad. Sci.* 1058:87.
2 Bayik, D., Gursel, I. and Klinman, D.M. 2016. Structure, mechanism and therapeutic utility of immunosuppressive oligonucleotides. *Pharmacol. Res.* 105:216.
3 Ishii, K. J., Gursel, I., Gursel, M. and Klinman, D. M. 2004. Immunotherapeutic utility of stimulatory and suppressive oligodeoxynucleotides. *Curr. Opin. Mol. Ther.* 6:166.
4 Krieg, A. M., Wu, T., Weeratna, R. *et al.* 1998. Sequence motifs in adenoviral DNA block immune activation by stimulatory CpG motifs. *Proc. Natl Acad. Sci. USA* 95:12631.
5 Gursel, I., Gursel, M., Yamada, H., Ishii, K. J., Takeshita, F. and Klinman, D. M. 2003. Repetitive elements in mammalian telomeres suppress bacterial DNA-induced immune activation. *J. Immunol.* 171:1393.
6 Klinman, D. M., Tross, D., Klaschik, S., Shirota, H. and Sato, T. 2009. Therapeutic applications and mechanisms underlying the activity of immunosuppressive oligonucleotides. *Ann. N. Y. Acad. Sci.* 1175:80.
7 Laplante, M. and Sabatini, D. M. 2012. mTOR signaling in growth control and disease. *Cell* 149:274.
8 Sengupta, S., Peterson, T. R. and Sabatini, D. M. 2010. Regulation of the mTOR complex 1 pathway by nutrients, growth factors, and stress. *Mol. Cell* 40:310.
9 Weichhart, T., Hengstschläger, M. and Linke, M. 2015. Regulation of innate immune cell function by mTOR. *Nat. Rev. Immunol.* 15:599.
10 Delgoffe, G. M., Kole, T. P., Zheng, Y. *et al.* 2009. The mTOR kinase differentially regulates effector and regulatory T cell lineage commitment. *Immunity* 30:832.
11 Vergadi, E., Ieronymaki, E., Lyroni, K., Vaporidi, K. and Tsatsanis, C. 2017. Akt signaling pathway in macrophage activation and M1/M2 polarization. *J. Immunol.* 198:1006.
12 Yang, Y. H., Dudoit, S., Luu, P. *et al.* 2002. Normalization for cDNA microarray data: a robust composite method addressing single and multiple slide systematic variation. *Nucleic Acids Res.* 30:e15.
13 Wright, G. W. and Simon, R. M. 2003. A random variance model for detection of differential gene expression in small microarray experiments. *Bioinformatics* 19:2448.

14 Klaschik, S., Tross, D., Shirota, H. and Klinman, D. M. 2010. Short- and long-term changes in gene expression mediated by the activation of TLR9. *Mol. Immunol.* 47:1317.
15 Klinman, D. M., Klaschik, S., Tomaru, K., Shirota, H., Tross, D. and Ikeuchi, H. 2010. Immunostimulatory CpG oligonucleotides: Effect on gene expression and utility as vaccine adjuvants. *Vaccine* 28:1919.
16 Klaschik, S., Gursel, I. and Klinman, D. M. 2007. CpG-mediated changes in gene expression in murine spleen cells identified by microarray analysis. *Mol. Immunol.* 44:1095.
17 Kaminski, J. J., Schattgen, S. A., Tzeng, T. C., Bode, C., Klinman, D. M. and Fitzgerald, K. A. 2013. Synthetic oligodeoxynucleotides containing suppressive TTAGGG motifs inhibit AIM2 inflammasome activation. *J. Immunol.* 191:3876.
18 Dodd, K. M. and Tee, A. R. 2015. STAT3 and mTOR: co-operating to drive HIF and angiogenesis. *Oncoscience* 2:913.
19 Hartman, H. N., Niemela, J., Hintermeyer, M.K. *et al.* 2015. Gain of function mutations of PIK3CD as a cause of primary sclerosing cholangitis. *J. Clin. Immunol.* 35:1.
20 Pourdehnad, M., Truitt, M. L., Siddiqi, I. N., Ducker, G. S., Shokat, K. M. and Ruggero, D. 2013. Myc and mTOR converge on a common node in protein synthesis control that confers synthetic lethality in Myc-driven cancers. *Proc. Natl Acad. Sci. USA* 110:11988.
21 Sarbassov, D. D., Ali, S. M., Kim, D. H. *et al.* 2004. Rictor, a novel binding partner of mTOR, defines a rapamycin-insensitive and raptor-independent pathway that regulates the cytoskeleton. *Curr. Biol.* 14:1296.
22 Finlay, D. K., Rosenzweig, E., Sinclair, L. V. *et al.* 2012. PDK1 regulation of mTOR and hypoxia-inducible factor 1 integrate metabolism and migration of $CD8^+$ T cells. *J. Exp. Med.* 209:2441.
23 Cho, J. H., Robinson, J. P., Arave, R. A. *et al.* 2015. AKT1 activation promotes development of melanoma metastases. *Cell Rep.* 13:898.
24 Tee, A. R., Blenis, J. and Proud, C. G. 2005. Analysis of mTOR signaling by the small G-proteins, Rheb and RhebL1. *FEBS Lett.* 579:21.
25 Freemerman, A. J., Johnson, A. R., Sacks, G. N. *et al.* 2014. Metabolic reprogramming of macrophages: glucose transporter (GLUT1)-mediated glucose metabolism drives a pro-inflammatory phenotype. *J. Biol. Chem.* 289:7884.
26 Delgoffe, G. M. and Powell, J. D. 2015. Feeding an army: the metabolism of T cells in activation, anergy, and exhaustion. *Mol. Immunol.* 68(2 Pt C):492.
27 Aagaard-Tillery, K. M. and Jelinek, D. F. 1994. Inhibition of human B lymphocyte cell cycle progression and differentiation by rapamycin. *Cell. Immunol.* 156:2.
28 Zhang, S., Readinger, J. A., DuBois, W. *et al.* 2011. Constitutive reductions in mTOR alter cell size, immune cell development, and antibody production. *Blood* 117:1228.
29 Lee, J. S., Vo, T. T. and Fruman, D. A. 2016. Targeting mTOR for the treatment of B cell malignancies. *Br. J. Clin. Pharmacol.* 82:1213.
30 Sackesen, C., van de Veen, W., Akdis, M. *et al.* 2013. Suppression of B-cell activation and IgE, IgA, IgG1 and IgG4 production by mammalian telomeric oligonucleotides. *Allergy* 68:593.